Kaleidoscope of quantum phases in a long-range interacting spin-1 chain

Z. -X. Gong,[1,2,*] M. F. Maghrebi,[1,2] A. Hu,[1,3] M. Foss-Feig,[1,2] P. Richerme,[1,4] C. Monroe,[1,2] and A. V. Gorshkov[1,2]

[1]*Joint Quantum Institute, NIST/University of Maryland, College Park, Maryland 20742, USA*
[2]*Joint Center for Quantum Information and Computer Science, NIST/University of Maryland, College Park, Maryland 20742, USA*
[3]*Department of Physics, American University, Washington, DC 20016, USA*
[4]*Department of Physics, Indiana University, Bloomington, Indiana, 47405, USA*

Motivated by recent trapped-ion quantum simulation experiments, we carry out a comprehensive study of the phase diagram of a spin-1 chain with XXZ-type interactions that decay as $1/r^\alpha$, using a combination of finite and infinite-size DMRG calculations, spin-wave analysis, and field theory. In the absence of long-range interactions, varying the spin-coupling anisotropy leads to four distinct phases: a ferromagnetic Ising phase, a disordered XY phase, a topological Haldane phase, and an antiferromagnetic Ising phase. If long-range interactions are antiferromagnetic and thus frustrated, we find primarily a quantitative change of the phase boundaries. On the other hand, ferromagnetic (non-frustrated) long-range interactions qualitatively impact the entire phase diagram. Importantly, for $\alpha \lesssim 3$, long-range interactions destroy the Haldane phase, break the conformal symmetry of the XY phase, give rise to a new phase that spontaneously breaks a $U(1)$ continuous symmetry, and introduce an exotic tricritical point with no direct parallel in short-range interacting spin chains. We show that the main signatures of all five phases found could be observed experimentally in the near future.

PACS numbers: 75.10.Jm, 75.10.Pq, 03.65.Vf, 05.30.Rt

arXiv:1510.02108v1 [cond-mat.str-el] 7 Oct 2015

The study of quantum phase transitions in low-dimensional spin systems has been a major theme in condensed matter physics for many years [1]. A well-known implication of Mermin and Wagner's famous results [2] on finite temperature quantum systems is that, for a large class of one-dimensional quantum spin systems, long-range order is forbidden even at zero temperature. This absence of classical order promotes quantum fluctuations to a central role, and they often determine the qualitative properties of the quantum ground state. An important example, first conjectured by Haldane [3, 4], is that a spin-1 antiferromagnetic Heisenberg chain possesses a disordered phase with an energy gap to bulk excitations, later identified as a symmetry protected topological phase [5, 6]. Its spin-1/2 counterpart, despite possessing the same classical limit, has a disordered ground state with gapless excitations, and is described by a conformal field theory (CFT) [7].

Experimentally, such quantum phase transitions have been explored in quasi-1D materials, and more recently using artificial materials designed through the careful control of atomic, molecular, and optical (AMO) systems [8–11]. These AMO systems are usually well-isolated from the environment, of system parameters, and make possible both measurement and control at the individual lattice-site level. A distinctive feature of AMO systems is that interactions between particles are often long-ranged, decaying as a power-law with distance ($1/r^\alpha$). The exponent α varies widely amongst different AMO systems, ranging from $\alpha = 6$ for van de Waals interactions in Rydberg atoms, to $\alpha = 3$ for polar molecules and magnetic atoms, to $\alpha = 0$ for atoms coupled to cavities [11–19]. The effect of long-range interactions can be tuned by either changing the dimensionality of the system, e.g. for neutral atoms or molecules in optical lattices, or by directly (and often continuously) altering the value of α, e.g. in trapped ions or cold atoms coupled to photonic crystals [14]. The availability of tunable long-range interactions creates an entirely new degree of freedom—absent in typical condensed-matter systems—for inducing quantum phase transitions, and can potentially lead to novel quantum phases [20–22].

While long-range interacting classical models have been studied in considerable detail for some time [23–27], there is a relative lack of in-depth studies of quantum phase transitions in long-range interacting systems, despite the emerging experimental prospects for studying both their equilibrium and non-equilibrium properties [15, 16, 18, 28–34]. One reason is that many analytically solvable lattice models become intractable when interactions are no longer short-ranged, a well-known example being the spin-1/2 XXZ model. In addition, to properly incorporate long-range interactions in low-energy effective theories, existing field theoretic treatments need to be modified and usually become much more complicated [35, 36]. Though numerically exact techniques for quantum systems have been adapted to treat long-range interactions, significant challenges remain in the numerical calculation of phase diagrams. In particular, power-law decaying interactions generally lead to a divergent correlation length [31, 37], and a much larger system size or a much higher precision is typically required to faithfully describe the properties of the system in the long-wavelength limit. Several authors have performed analytical studies of non-interacting bosonic and fermionic systems with long-range hopping and pairing [32, 34, 38, 39], but there have been relatively few numerical studies of non-integrable systems, and those that exist have primarily focused on spin-1/2 chains [20, 28, 40–42].

In this manuscript, we carry out a detailed study of a spin-1 chain with tunable XXZ interactions that decay monotonically as $1/r^\alpha$, for all $\alpha > 0$. Our study is largely motivated by imminent trapped-ion based experiments that can simulate this model with widely tunable index α [43–45]. In the absence of long-range interactions, the choice of spin-1 over spin-1/2 allows us to have four distinct quantum phases by

varying the anisotropy of the interactions: a ferromagnetic (FM) phase and an antiferromagnetic (AFM) Ising phase that are both gapped and long-range ordered, a disordered gapless phase (the XY phase), and a gapped and topologically ordered phase (the Haldane phase). By using a combination of density matrix renormalization group (DMRG) calculations, spin wave analysis, and field theory, we obtain the phase diagram for arbitrary anisotropy and all $\alpha > 0$, with both ferromagnetic and antiferromagnetic interactions. Our key observation is that, when interactions in all spatial directions are antiferromagnetic, long-range interactions are frustrated, leading to primarily quantitative changes to the phase boundaries compared to the short-range interacting chain. Interestingly, we find that the topological Haldane phase is robust under long-range interactions with any $\alpha > 0$ [46]. However, when the interactions in the $x-y$ plane become ferromagnetic, we find a number of significant modifications to the phase diagram: (1) The Haldane phase is destroyed at a finite α due to a closing of the bulk excitation gap; (2) The gapless XY phase, described by a CFT with central charge $c = 1$, disappears when $\alpha \lesssim 3$ due to a breakdown of conformal symmetry [32, 34]; (3) The disappearance of the XY phase heralds the emergence of a new phase at $\alpha \lesssim 3$ (continuous-symmetry breaking, or CSB) in which the spins order in the xy plane, spontaneously breaking a $U(1)$ symmetry and possessing gapless excitations (Nambu-Goldstone modes); (4) Novel tricritical points, with no direct analogue in short-range interacting 1D models, appear at the intersection of the Haldane, CSB, and XY/AFM phases.

The manuscript is organized as follows. In Sec. I, we introduce the model Hamiltonian and present complete phase diagrams for the ferromagnetic and antiferromagnetic cases. In Sec. II, we study the boundary of the FM phase, where a spin-wave approximation is found to be asymptotically exact in the large-system limit. In Sec. III, we determine both the XY-to-Haldane and Haldane-to-AFM transition lines accurately using DMRG calculations, and use field theory arguments to explain the effect of long-range interactions on the boundary of the Haldane phase. In Sec. IV, we introduce the new CSB phase and explain its emergence using spin-wave theory. The boundary between the CSB and XY phases is determined by a numerical calculation of central charge. In Sec. V, we show that all five phases possess distinct signatures that could be observed in near-future trapped ion quantum simulations with chains of 16 spins. Finally, we conclude the work in Sec. VI and comment on a number of open questions.

I. MODEL HAMILTONIAN AND PHASE DIAGRAMS

We consider the following spin-1 Hamiltonian with long-range XXZ interactions in a 1D open-boundary chain:

$$H = \sum_{i>j} \frac{1}{(i-j)^\alpha} [J_{xy}(S_i^x S_j^x + S_i^y S_j^y) + J_z S_i^z S_j^z]. \quad (1)$$

Here $J_z \in (-\infty, \infty)$ and $\alpha \in (0, \infty)$ are allowed to vary continuously, and we consider both the $J_{xy} = 1$ (antiferromagnetic) and $J_{xy} = -1$ (ferromagnetic) cases. We note that, for $0 < \alpha < 1$, Eq. (1) does not have a well-defined thermodynamic limit when J_{xy} and/or J_z is ferromagnetic, since the ground-state energy-density diverges. To make the ground-state energy extensive, we may impose an energy renormalization factor $N^{\alpha-1}$, first introduced by Kac [47], when taking the thermodynamic or continuum limit (here N is the chain length). For finite-size numerical calculations, we do not need to implement the Kac renormalization for $0 < \alpha < 1$ since ground-state properties are unaffected by energy renormalization [48].

Figure 1 shows our full phase diagram for both $J_{xy} = 1$ and $J_{xy} = -1$, with actual phase boundaries plotted using the results of calculations discussed in the following sections. The nearest-neighbor interaction limit is achieved at $\alpha \to \infty$ ($1/\alpha = 0$). In this limit, the Hamiltonian in Eq. (1) with $J_{xy} = -1$ is equivalent to the one with $J_{xy} = 1$, as can be seen by performing a local unitary transformation that flips every other spin in the $x-y$ plane while preserving the spin commutation relations: $S_i^{x,y} \to (-1)^i S_i^{x,y}$. The different ground-state phases of this short-range Hamiltonian have been well-studied [49–51]. Notably, Haldane first conjectured [3, 4] that for $\lambda_1 < J_z < \lambda_2$, a disordered gapped phase (the Haldane phase) will emerge. At $J_z = \lambda_2$, the ground state undergoes a second-order phase transition from the Haldane phase to an AFM phase, which belongs to the same universality class as the 2D Ising model. The value $\lambda_2 \approx 1.186$ has been found by various numerical techniques including Monte-Carlo [52], exact diagonalization [53], and DMRG [54–56]. At $J_z = \lambda_1$, a Berezinskii-Kosterlitz-Thouless (BKT) transition intervenes between the Haldane phase and a gapless disordered XY phase at $J_z < \lambda_1$. The value of λ_1 is theoretically predicted to be exactly zero after mapping Eq. (1) (for $\alpha = \infty$) to a field theory model using bosonization [57]. This prediction is supported by conformal field theory arguments [58] and a level spectroscopy method based on a renormalization group analysis and the $SU(2)/Z_2$ symmetry of the BKT transition [50, 59–61]. Numerically, $\lambda_1 \approx 0$ has been verified via finite-size scaling [53, 62, 63] and DMRG [54]. Finally, at $J_z = \lambda_0 = -1$, a first-order phase transition from the XY phase to a ferromagnetic Ising phase takes place [50, 55, 64].

We now introduce our results for the long-range interacting case ($1/\alpha > 0$). For $J_{xy} = 1$ and $J_z > 0$, long-range interactions are frustrated and the Haldane-to-AFM phase transition point $\lambda_2(\alpha)$ increases moderately as α decreases, without changing the universality class of the transition. For sufficiently small $J_z < 0$, the ferromagnetic long-range interactions along the z direction eventually favor a ferromagnetic ground state, inducing a first-order transition at $\lambda_0(\alpha)$. The magnitude of the critical coupling, $|\lambda_0(\alpha)|$, decreases monotonically from 1 (at $\alpha = \infty$) to 0 (for all $\alpha \leq 1$) in the thermodynamic limit. The XY-to-Haldane phase boundary $\lambda_1(\alpha)$ becomes negative for finite α, similar to the XXZ spin-1 chain with next-nearest-neighbor interactions [65], eventu-

ally terminating in a tricritical point at the intersection of FM, Haldane, and XY phases. The entire XY phase (including the XY-to-Haldane phase boundary) has conformal symmetry with $c = 1$, and the XY-to-Haldane phase boundary remains a BKT transition until it terminates at the tricritical point.

For $J_{xy} = -1$, where long-range interactions in the $x - y$ plane are not frustrated, the phase diagram [Fig. 1(b)] shows a number of important qualitative differences from the nearest-neighbor phase diagram as α is decreased. First, the XY-to-Haldane phase boundary bends significantly toward positive J_z, and we find the Haldane phase to terminate at $\alpha \approx 3$ for $J_z = 1$. Second, we expect the XY phase to disappear for $\alpha \lesssim 3$ due to the breakdown of conformal symmetry [32, 34]. Third, for $\alpha \lesssim 3$ a new CSB phase emerges—this is not in violation of the Mermin-Wagner theorem, as it no longer applies for this range of interactions [2, 40, 66–69]. The CSB-to-AFM phase transition is expected to be first-order, since at large J_z and small α, quantum fluctuations play negligible roles for both the Néel-ordered state and the ordered CSB state. This behavior is similar to the transition between the AFM phase and the large-D phase (where a large positive anisotropy term $D\sum_i (S_i^z)^2$ causes all spins to stay in the $|S_i^z = 0\rangle$ state) reported in Refs. [54, 55, 64]. The Haldane phase has a $c = 1$ critical phase boundary with the XY phase, a $c = 0.5$ phase boundary with the AFM phase [56], and a possibly exotic phase boundary with the CSB phase, a boundary that is not described by a 1+1D CFT.

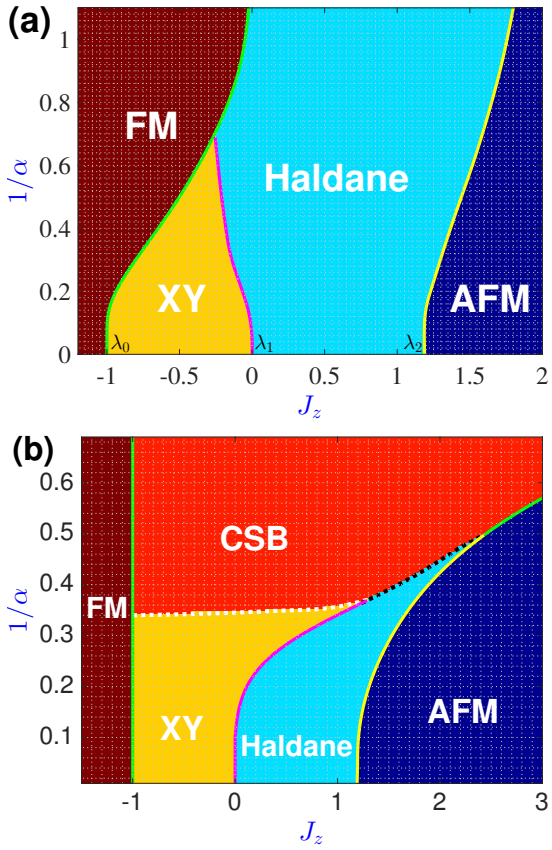

Figure 1: Proposed phase diagram for (a) $J_{xy} = 1$ and (b) $J_{xy} = -1$. Five different phases are identified: a ferromagnetic (FM) Ising phase, an antiferromagnetic (AFM) Ising phase, a disordered XY phase, a topological Haldane phase, and a continuous symmetry breaking (CSB) phase. At $\alpha = \infty$, the transition points are denoted by $J_z = \lambda_{0,1,2}$ in (a). The FM-to-XY, FM-to-CSB, and CSB-to-AFM transitions are first order (green line); the XY-to-Haldane transition is BKT type with central charge $c = 1$ (purple line); the Haldane-to-AFM transition is second order with $c = 0.5$ (yellow line); the CSB-to-XY transition (white dashed line) has $c = 1$, but is a BKT-like transition corresponding to a universality class different from the XY-to-Haldane transition [69]; the CSB-to-Haldane transition (black dashed lines) appears to be an exotic continuous phase transition not described by a 1+1D CFT. The location of solid transition lines are expected to be accurate in the thermodynamic limit, while the location of dashed transition lines may be inaccurate due to finite-size effects in our numerics.

II. FM PHASE AND ITS BOUNDARY

Because the ferromagnetic state with all spins polarized along $\pm z$ (or an arbitrary superposition of these two states) is an exact eigenstate of the Hamiltonian for any value of α and J_z, we expect a first-order quantum phase transition at the boundary of the FM phase. The FM state has an energy $E_{\rm FM} = J_z \sum_{i>j} (i-j)^{-\alpha}$, and the phase transition out of this state, defining the critical line $J_z = \lambda_0(\alpha)$, occurs when some other eigenstate with no ferromagnetic order appears with a lower energy. The dependence of λ_0 on α can be estimated using the following intuitive argument. For a given $J_z < 0$, the energy density of the ferromagnetic state in the thermodynamic limit is given by $\epsilon_{\rm FM} = J_z \zeta(\alpha)$ [$\zeta(\alpha) \equiv \sum_{r=1}^{\infty} r^{-\alpha}$ is the Riemann zeta function], which diverges as $\alpha \to 1$. For $J_{xy} = 1$, the magnitude of the energy density arising from the term $\sum_{i>j} (S_i^x S_j^x + S_i^y S_j^y)/(i-j)^\alpha$ can be at most $\eta(\alpha) \equiv \sum_{r=1}^{\infty} (-1)^{r-1}/r^\alpha$ (the Dirichlet eta function), with this value obtained for any state that is Néel-ordered along some direction in the $x - y$ plane. The competition between the energy of these two classical states gives a critical point $J_z \approx -\eta(\alpha)/\zeta(\alpha)$, which smoothly varies from $J_z = -1$ at $\alpha = \infty$ to $J_z = 0$ at $\alpha = 1$. For $J_{xy} = -1$, the situation is quite different, because the polarized state along any direction in the $x - y$ plane has an energy density equal to $-\zeta(\alpha)$, and thus we naively expect the phase boundary to be at $J_z = -1$ for all $\alpha > 0$.

More formally, the boundary can be calculated via a spin-wave analysis. We treat the spin state that is polarized along the $+z$ direction as the vacuum state with no excitations, and apply the Holstein-Primakoff transformation (for spin 1) to map spin excitations (spin-waves) into bosons: $S_i^z = 1 - a_i^\dagger a_i$, $S_i^+ \equiv S_i^x + i S_i^y = \sqrt{2} a_i^\dagger (1 - a_i^\dagger a_i/2)^{1/2}$. In the weak excitation limit, $\langle a_i^\dagger a_i \rangle \ll 1$, we can approximate $S_i^+ \approx \sqrt{2} a_i^\dagger$, and our Hamiltonian becomes

$$H_{\rm sw} \approx \sum_{i>j} \frac{-J_z (a_i^\dagger a_i + a_j^\dagger a_j) + J_{xy} (a_i^\dagger a_j + a_j^\dagger a_i)}{(i-j)^\alpha}, \quad (2)$$

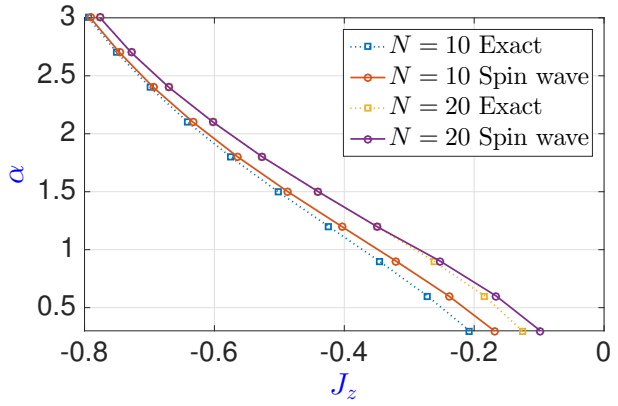

Figure 2: Comparison of the (first-order) transition point out of the FM phase calculated using finite-size DMRG and spin-wave theory for $J_{xy} = 1$. The DMRG result is regarded as exact since its error is far below the resolution of the plot.

where we have ignored the interaction terms $a_i^\dagger a_i a_j^\dagger a_j$ since $\langle a_i^\dagger a_i\rangle, \langle a_j^\dagger a_j\rangle \ll 1$ is assumed. Assuming for the moment periodic boundary conditions, this quadratic Hamiltonian can be diagonalized by Fourier transformation, $H_{\rm sw} = 2\sum_k \omega_k c_k^\dagger c_k$, with the following dispersion relation ($q \equiv 2\pi k/N$) for an infinite system

$$\omega(q) = -J_z \sum_{r=1}^{\infty} r^{-\alpha} + J_{xy} \sum_{r=1}^{\infty} \cos(qr)/r^{\alpha}. \qquad (3)$$

If $\omega_{min} \equiv \min \omega(q) > 0$, then the ground state of $H_{\rm sw}$ is the vacuum state of all modes k, and $\langle a_i^\dagger a_i\rangle = 0$ for all i, consistent with the approximation $\langle a_i^\dagger a_i\rangle \ll 1$. If $\omega_{min} < 0$, then the ground state has an extensive number of spin excitations and the spin-wave approximation should break down, and we do not expect the polarized state in the z direction to be the quantum ground state. The $\omega_{min} = 0$ condition thus sets the phase boundary for $H_{\rm sw}$. For $J_{xy} = 1$, $\omega_{min} = \omega(q = \pi) = -J_z\zeta(\alpha) - \eta(\alpha)$, leading to a critical line of $J_z = -\eta(\alpha)/\zeta(\alpha)$. For $J_{xy} = -1$, $\omega_{min} = \omega(q = 0) = (1 - J_z)\zeta(\alpha)$, leading to a critical line at $J_z = -1$, independent of α. These results exactly match with the previous intuitive arguments.

Note that we can estimate the transition point of a finite chain without translational invariance by numerically diagonalizing $H_{\rm sw}$. However, we note that the spin-wave analysis is not necessarily exact in this case. The interactions between bosons that we have ignored can make multi-particle eigenstates have a lower energy than the vacuum state, despite the fact that the single-particle excitation spectrum has a finite-size gap. In other words, the condition $\omega_{min} > 0$ only guarantees the ferromagnetic state to be the ground state of the non-interacting Hamiltonian $H_{\rm sw}$ [Eq. (2)], but not of the original Hamiltonian [Eq. (1)]. This effect of interactions can indeed be observed for finite-size systems. In Fig. 2, we show that for $J_{xy} = 1$, the critical J_z obtained by exact numerical calculations of Eq. (1) with $N = 10$ spins is slightly smaller than spin-wave prediction given by the condition $\omega_{min} = 0$ for $0 < \alpha < \infty$. To the contrary, for $J_{xy} = -1$ we find that the spin-wave prediction is exact for any number of spins and for all $\alpha > 0$.

It is also interesting to note that the deviation of the transition point due to the spin-wave approximation decreases with increasing α, and vanishes in the $\alpha \to \infty$ limit, showing that long-range interactions are playing an important role. However, using a finite-size DMRG algorithm [70–73], we find that as N increases, the deviation caused by the spin-wave approximation decreases quickly (Fig. 2). In addition, by using an infinite-size DMRG algorithm [73, 74], we find that the spin-wave prediction of the transition line $J_z = -\eta(\alpha)/\zeta(\alpha)$ [the green line in Fig. 3(a)] is correct within our numerical precision, strongly suggesting that the spin-wave prediction becomes exact in the thermodynamic limit.

III. HALDANE PHASE AND ITS BOUNDARY

The existence of the Haldane phase in a spin-1 XXZ chain makes the phase diagram much richer than that of a spin-1/2 XXZ chain. We focus first on the XY-to-Haldane phase boundary $\lambda_1(\alpha)$. The transition out of the Haldane phase is signaled by a vanishing of the string-order correlation function $\mathcal{S}_{ij}^{\xi} \equiv \langle S_i^{\xi} S_j^{\xi} \prod_{i<k<j} (-1)^{S_k^{\xi}}\rangle$ ($\xi = x, y, z$) when $|i - j| \to \infty$. However, because the phase transition is of the BKT type, $\mathcal{S}_{ij}^{\xi}$ changes rather smoothly with J_z and α for a finite $|i - j|$, and it is very challenging to find the exact transition point numerically. Finite-size scaling using exact diagonalization on small chains must be performed very carefully due to logarithmic corrections in system size [50, 75–77], and infinite-size DMRG yields a phase transition point that depends strongly on the bond dimension χ (the dimension of the matrix product states used [70]), since the ground state bipartite entanglement entropy S grows logarithmically with system size N according to CFT: $S = c \log N + \text{const}$ [78]. As seen in Fig. 3, for $\chi = 100$ and at $\alpha = \infty$, the string-order correlation function $\mathcal{S}_{ij}^{z}$ appears to start vanishing at $J_z \approx 0.3$, instead of at $J_z = 0$ as predicted by field theory [57]. However, this is consistent with previous infinite-size DMRG calculation results [54, 55]. To extract a more accurate phase boundary, we perform a scaling of χ ranging from 50 to 200 near the XY-to-Haldane phase boundary, following a procedure similar to that in Ref. [54]. We then extract the XY-to-Haldane phase boundary (white line in Fig. 3) by determining the location where $\mathcal{S}_{ij}^{z}(\chi \to \infty)$ vanishes, which now correctly yields $J_z \approx 0$ at $\alpha = \infty$. However, we expect a few percent uncertainty in the transition point due the use of $\mathcal{S}_{ij}^{z}$ at a finite separation $|i - j|$, and due to the error in extrapolating $\mathcal{S}_{ij}^{z}(\chi \to \infty)$.

To explain why long-range interactions bend the XY-to-Haldane phase boundary in opposite directions for ferromagnetic and antiferromagnetic J_{xy}, we use an effective field theory first proposed by Haldane [3] and developed by Af-

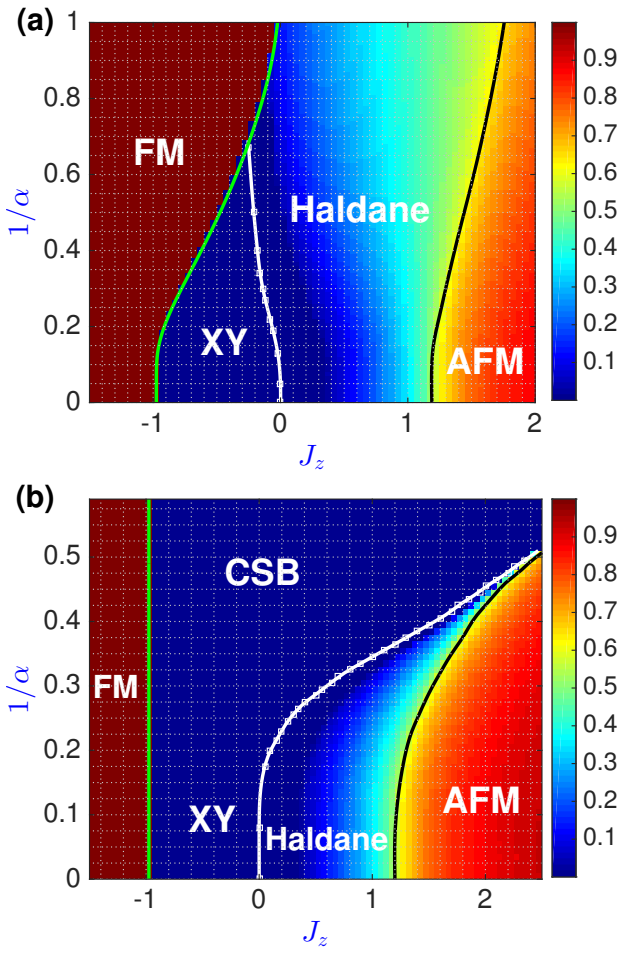

Figure 3: Infinite-size DMRG calculation of $\mathcal{S}^z_{ij} \equiv \langle S^z_i S^z_j \prod_{i<k<j}(-1)^{S^z_k}\rangle$ for a separation of $|i-j| = 500$. $\mathcal{S}^z_{ij} = 1$ in the FM phase and $\mathcal{S}^z_{ij} \approx 1$ deep in the AFM phase for any i and j. As $|i-j| \to \infty$, $\mathcal{S}^z_{ij}$ is finite for the Haldane phase and zero for the XY phase, thus we can use it to locate the XY-to-Haldane phase boundary. (a) $J_{xy} = 1$. The FM phase boundary (green line) is given by the spin-wave prediction $J_z = -\eta(\alpha)/\zeta(\alpha)$. (b) $J_{xy} = -1$. The FM phase boundary (green line) is exactly at $J_z = -1$. For both (a) and (b), we vary the bound dimension χ to accurately determine the XY-to-Haldane phase boundary, determining the value of J_z at which $\mathcal{S}^z_{ij}$ vanishes (for a large but finite $|i-j|$) and then extrapolating to the $\chi \to \infty$ limit (white squares fitted by the white line). The black line is the Haldane-to-AFM phase boundary, which is determined from $\langle S^z_i S^z_j\rangle$ (see text) and which converges well within the resolution of the plot for $\chi \geq 100$.

fleck [79]. The proper inclusion of long-range interactions within this field theoretic approach was discussed in detail in Ref. [46]. Here, we give a brief review of this field-theory treatment. Consider first the case of $J_{xy} = J_z = 1$. In this case, each spin-1 is mapped to a staggered field $\boldsymbol{n}(2i+\frac{1}{2}) = (\boldsymbol{S}_{2i} - \boldsymbol{S}_{2i+1})/2$ and a uniform field $\boldsymbol{l}(2i+\frac{1}{2}) = (\boldsymbol{S}_{2i} + \boldsymbol{S}_{2i+1})/2$. Importantly, we observe that the classical ground state of H is always Néel-ordered for any $\alpha > 0$, with $\boldsymbol{n}^2(x) = 1$ and $\boldsymbol{l}(x) = 0$ for any position x. The intuition behind this decomposition is that, in the quantum ground state, $\boldsymbol{n}(x)$ should have only long-wave-length variations with $\boldsymbol{n}^2(x) \approx 1$, while $\boldsymbol{l}(x) \approx 0$ should represent long wave-length perturbations to the direction of $\boldsymbol{n}(x)$ due to quantum fluctuations. Therefore, when working with the Fourier-transformed fields $\boldsymbol{n}(q)$ and $\boldsymbol{l}(q)$, we can expand the Hamiltonian in powers of the momentum q and keep only the leading order terms.

The effective Hamiltonian in the continuum limit and momentum space reads

$$H_{\text{eff}} \approx \int dq \left[\omega(q)|\boldsymbol{n}(q)|^2 + \Omega(q)|\boldsymbol{l}(q)|^2\right], \tag{4}$$

where the cross terms between $\boldsymbol{n}$ and $\boldsymbol{l}$ are ignored because they involve $\boldsymbol{n}(q)$ near $q = \pi$. The dispersion relations $\Omega(q)$ and $\omega(q)$ can be expanded at small q as [80]:

$$\begin{aligned}
\omega(q) &\equiv 2\sum_{r=1}^{\infty}(-1)^r \frac{\cos(qr)}{r^\alpha} \approx -2\eta(\alpha) + \eta(\alpha-2)q^2 + O(q^4), \\
\Omega(q) &\equiv 2\sum_{r=1}^{\infty}\frac{\cos(qr)}{r^\alpha} \approx 2\zeta(\alpha) + \zeta(\alpha-2)q^2 + O(q^4) \\
&\quad + 2\Gamma(1-\alpha)\cos[\frac{\pi}{2}(\alpha-1)]|q|^{\alpha-1}.
\end{aligned} \tag{5}$$

For the $\boldsymbol{n}$ field, we need to keep the q^2 term since the zeroth-order term gives a constant due to the approximation $\boldsymbol{n}^2(x) \approx 1$. The zeroth-order term in q for the $\boldsymbol{l}$ field is the dominant source of quantum fluctuations, and we can ignore higher-order terms in determining whether H_{eff} is gapped or not (they do contribute to the long-distance behavior of correlation functions though [46]). Because H_{eff} is quadratic in both fields, we can first integrate out the $\boldsymbol{l}$ field using the standard coherent spin-state path integral [1]. We then obtain a 1D O(3) nonlinear sigma model (NLSM) of the field $\boldsymbol{n}$ [3], which can be treated by removing the nonlinear constraint $\boldsymbol{n}^2 = 1$ while phenomenologically introducing a gap Δ_α and a renormalized spin-wave velocity v_α [46, 81]. We thereby arrive at a free field theory with the Lagrangian density (written in momentum space)

$$\mathcal{L}(q) \propto \left(\frac{\partial \boldsymbol{n}}{\partial t}\right)^2 - (\Delta_\alpha^2 + v_\alpha^2 q^2)|\boldsymbol{n}(q)|^2. \tag{6}$$

The existence of the gap can be understood by the renormalization group flow of the coupling strength [1, 82], or by considering the SU(n) variant of the Hamiltonian, for which the corresponding O(n) NLSM can be solved analytically in the $n \to \infty$ limit and give rise to a mass gap [79, 83]. We infer that Δ_α should increase as α decreases, since $\Delta_{\alpha\to\infty} \approx 0.41$ [84, 85] and $\Delta_{\alpha\to 0} = 1$ (where the Hamiltonian becomes integrable). This speculation is confirmed by accurate finite-size DMRG calculation of Δ_α [46].

Next, we consider the case of $J_{xy} = 1$ but $J_z < 1$. We can then write

$$H = \sum_{i>j}\frac{1}{(i-j)^\alpha}\boldsymbol{S}_i \cdot \boldsymbol{S}_j - (1-J_z)\sum_{i>j}\frac{1}{(i-j)^\alpha}S^z_i S^z_j. \tag{7}$$

Following Refs. [79, 86], the anisotropy term above can be treated as a negative mass term $(1-J_z)f_\alpha n_z^2(q)$ to the Lagrangian density $\mathcal{L}(q)$ in Eq. (6). The precise value of the renormalization factor f_α is not important to us, but we expect it to continuously decrease as α becomes smaller, since the staggered field dominates in the Haldane phase and long-range interactions [$\sum_{i>j}\frac{1}{(i-j)^\alpha}S_i^zS_j^z$ in Eq. (7)] are increasingly frustrated as α decreases. The mass gap for the field n_z is now smaller than for n_x and n_y, and reads $\Delta_\alpha(J_z)=\sqrt{\Delta_\alpha^2-(1-J_z)f_\alpha}$. Combined with the above discussion that Δ_α should increase with decreasing α, we require progressively more negative J_z to close the gap and transition into the XY phase as α decreases, thus explaining the shape of the XY-to-Haldane phase boundary in Fig. 3(a).

For $J_{xy}=-1$ and $J_z<1$, the classical ground state is no longer Néel ordered and the field theory employed above is not valid. However, by rotating every other spin by π about the z-axis, we generate a transformed Hamiltonian

$$H'=\sum_{i>j}\frac{(-1)^{i-j-1}}{(i-j)^\alpha}\boldsymbol{S}_i\cdot\boldsymbol{S}_j+\sum_{i>j}\frac{J_z-(-1)^{i-j-1}}{(i-j)^\alpha}S_i^zS_j^z. \tag{8}$$

Now the classical ground state *is* Néel ordered (along any direction for $J_z=1$). The first term above is isotropic, and gets mapped to

$$\sum_{i>j}\frac{(-1)^{i-j-1}}{(i-j)^\alpha}\boldsymbol{S}_i\cdot\boldsymbol{S}_j\approx\int dq\left[\Omega(q)|\boldsymbol{n}(q)|^2+\omega(q)|\boldsymbol{l}(q)|^2\right], \tag{9}$$

where the roles of $\omega(q)$ and $\Omega(q)$ are swapped as compared to Eq. (4). For $\alpha<3$, $\Omega(q)$ in Eq. (5) is now dominated by the non-analytic term $|q|^{\alpha-1}$ at small q, and we can no longer obtain the simple free Lagrangian in Eq. (6). In Ref. [46], it is shown that the $|q|^{\alpha-1}$ term in the dispersion of $\boldsymbol{n}(q)$ in Eq. (9) leads to a renormalization group flow towards a gapless ordered phase spontaneously breaking an $SU(2)$ symmetry for $\alpha<\alpha_c\lesssim 3$. For our complete Hamiltonian H' in Eq. (8), the anisotropy leads instead to a $U(1)$ continuous symmetry breaking phase for $\alpha<\alpha_c'$ (see the next section for further discussions, where α_c' is estimated to be 2.9 at $J_z=1$). Our infinite-size DMRG calculations in Fig. 3(b) suggest that the Haldane phase terminates at a critical α around 3.1 for $J_z=1$, and the XY phase is expected to exist in between the CSB phase and the Haldane phase at $J_z=1$.

For $\alpha>3$, $\Omega(q)$ is dominated by q^2 and we can once again reduce H' to the free field Lagrangian Eq. (6), but with a different mass gap Δ_α' and spin-wave velocity v_α'. The anisotropy term in Eq. (8) changes the gap to $\Delta_\alpha'(J_z)=\sqrt{\Delta_\alpha'^2-(g_\alpha-J_zh_\alpha)}$. Here g_α is a renormalization factor due to non-frustrating long-range interactions $\frac{(-1)^{i-j-1}}{(i-j)^\alpha}S_i^zS_j^z$ in Eq. (8), and should thus increase as α decreases, while h_α is a renormalization factor due to frustrating long-range interaction $\frac{1}{(i-j)^\alpha}S_i^zS_j^z$ in Eq. (8), and should decrease as α decreases. Together with the expectation that the gap Δ_α' should decrease with α [46] due to the appearance of gapless continuous symmetry breaking phase at $\alpha\lesssim 3$, we conclude that the gap closes at a point with J_z strictly larger than zero in the presence of long-range interactions, again consistent with our numerical results.

We point out that a different field theoretic approach based on non-Abelian bosonization [46, 57] can also be employed to predict the qualitative changes to the XY-to-Haldane phase boundary. This technique has been used to predict the XY-to-Haldane phase boundary of a spin-1 XXZ chain with next-nearest-neighbor interactions [86], which is a reasonable approximation to our model when α is large enough that next-nearest-neighbor interactions dominate over the next-longer-range interactions.

We end this section with a brief discussion of the boundary between the Haldane and AFM phases. Both the Haldane and AFM phases are gapped and have finite entanglement entropy in the infinite-system-size limit [87]. Thus our infinite-size DMRG calculations should precisely reproduce the phase boundary between the two phases; indeed we see well-converged results for bond dimensions of $\chi\geq 100$. We extract the Haldane-to-AFM phase boundaries using the spin-spin correlation functions $C_{ij}^z\equiv\langle S_i^zS_j^z\rangle$ (not shown), and plot them as black lines in Figs. 3(a,b). The bending of the Haldane-to-AFM phase boundary toward larger J_z for both $J_{xy}=1$ and $J_{xy}=-1$ in the presence of long-range interactions can be understood via simple energetic considerations. In the AFM phase, the spins are (nearly) anti-aligned in the z direction; long-range interactions are strongly frustrated, and the energy $E=\sum_{i>j}\langle S_i^zS_j^z\rangle/(i-j)^\alpha$ at $\alpha\to 0$ is only half of the $\alpha=\infty$ case for a perfectly Néel ordered state. In the Haldane phase, the AFM order of spin correlations $\langle\boldsymbol{S}_i\cdot\boldsymbol{S}_j\rangle$ decays exponentially (followed by a small power-law tail [46]), and thus the ground state energy $E=\sum_{i>j}\langle\boldsymbol{S}_i\cdot\boldsymbol{S}_j\rangle/(i-j)^\alpha$ is much less frustrated by the long-range interactions. As a result, we expect the disordered ground state in the Haldane phase to have progressively lower energy than an AFM ordered state as α decreases at a given J_z, and hence a larger (but always finite even for $\alpha\to 0$) J_z is needed to make the transition from the Haldane phase into the AFM phase.

IV. CSB PHASE AND ITS BOUNDARY

The celebrated Mermin-Wagner theorem rigorously rules out continuous symmetry breaking in 1D and 2D quantum and classical spin systems at finite temperature, as long as the interactions satisfy the convergence condition $\sum_{i>j}J_{ij}r_{ij}^2<\infty$ in the thermodynamic limit (r_{ij} and J_{ij} are respectively the distance and coupling strength between sites i and j) [2]. The long-distance properties of 1D spin systems at zero temperature can often be related to those of a 2D classical model at finite temperature; however, in the process of this mapping, the long-range interactions are only inherited by one of the two spatial directions in the classical model, and the Mermin-Wagner convergence condition will be satisfied for interac-

tions decaying faster than $1/r^3$. Thus we expect no continuous symmetry breaking in the ground state of our Hamiltonian Eq. (1) for $\alpha > 3$. Indeed, we have found exclusively disordered or discrete (Z_2) symmetry breaking phases for $\alpha > 3$ in our phase diagrams (Fig. 1). Continuous symmetry breaking can (and does) appear when $\alpha < 3$. To gain a better understanding of the robustness of symmetry breaking states to quantum fluctuations, below we carry out a spin-wave analysis [88].

We start by considering the $J_{xy} = -1$ case, and take the state with all spins polarized along the $+x$ direction as the vacuum state. With this choice of vacuum, and assuming that the density of spin waves is small ($\langle a_i^\dagger a_i\rangle \ll 1$ in the following expressions), the Holstein-Primakoff mapping is now $S_i^x = 1 - a_i^\dagger a_i$, $S_i^y \approx (a_i^\dagger + a_i)/\sqrt{2}$, $S_i^z \approx (a_i^\dagger - a_i)/i\sqrt{2}$. Under this mapping, and dropping terms that are quartic in bosonic operators (again based on the assumption that $\langle a_i^\dagger a_i\rangle \ll 1$), H becomes

$$H_{\text{swx}} = \sum_{k=-N/2}^{N/2} \begin{pmatrix} a_k^\dagger & a_{-k} \end{pmatrix} \begin{pmatrix} \omega_k & \mu_k \\ \mu_k & \omega_k \end{pmatrix} \begin{pmatrix} a_k \\ a_{-k}^\dagger \end{pmatrix}; \quad (10)$$

$$\omega_k = \sum_{r=1}^{N/2} J_r + \frac{J_z - 1}{2} \sum_{r=1}^{N/2} J_r \cos(\frac{2\pi k}{N} r), \quad (11)$$

$$\mu_k = -\frac{J_z + 1}{2} \sum_{r=1}^{N/2} J_r \cos(\frac{2\pi k}{N} r), \quad (12)$$

where $a_k = \frac{1}{\sqrt{N}} \sum_j e^{i2\pi jk/N} a_j$. H_{swx} can be diagonalized with a Bogoliubov transformation, yielding non-interacting Bogoliubov quasi-particles with a spectrum ν_k. Importantly, when $|\omega_k| > |\mu_k|$, $\nu_k > 0$ and the vacuum is dynamically stable. When $|\omega_k| < |\mu_k|$, ν_k is imaginary and the system is dynamically unstable indicating that we have made the wrong choice of a classical ground state. Using the expressions for ω_k and μ_k in Eqs. (11) and (12), we find that $|\omega_k| > |\mu_k|$ is satisfied for all $k \neq 0$ modes if and only if $-1 \leq J_z < \zeta(\alpha)/\eta(\alpha)$. This is because when $J_z < -1$, the classical ground state is ferromagnetic in z direction, and when $J_z > \zeta(\alpha)/\eta(\alpha)$ the classical ground state is Néel ordered along the z direction.

Because the Bogoliubov quasiparticles consist of both particles and holes, the ground state of H_{swx} can have a finite or even divergent density of spin excitations, measured by

$$\langle a_i^\dagger a_i\rangle = \frac{1}{N} \sum_{k\neq 0} \frac{1}{2}([1 - \mu_k^2/\omega_k^2]^{-1/2} - 1) \quad (13)$$

$$\xrightarrow{N\to\infty} \frac{1}{4\pi} \int_{-\pi}^{\pi} dq \left([1 - \mu^2(q)/\omega^2(q)]^{-1/2} - 1\right).$$

The integrand $[1 - \mu^2(q)/\omega^2(q)]^{-1/2}$ above diverges at $q = 0$, and whether or not the integral is infrared divergent depends on the value of α. We find that for $\alpha > 3$, $[1 - \mu^2(q)/\omega^2(q)]^{-1/2} \propto |q|^{-1}$ to leading order in q, and therefore $\langle a_i^\dagger a_i\rangle \sim \ln(N)$ diverges as $N \to \infty$. This means

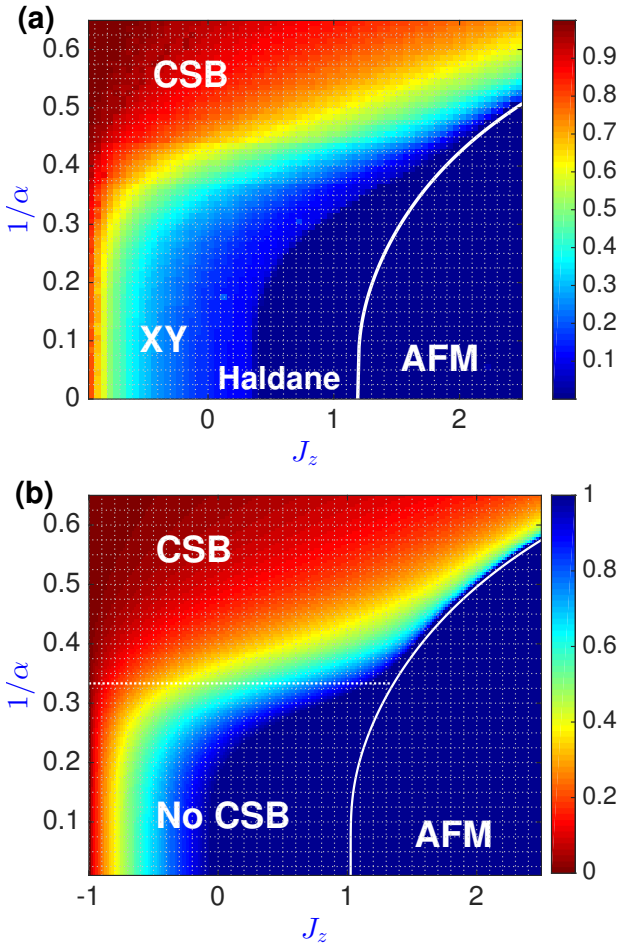

Figure 4: Continuous symmetry breaking for $J_{xy} = -1$. (a) iDMRG calculation of $\langle S_i^+ S_j^-\rangle$ for $|i - j| = 500$, with bond dimension $\chi = 200$ (at this separation and bond dimension, the results are well converged). Long-range order in the $x - y$ plane is increasingly favored as α decreases, but we can not extract a sharp phase boundary between the CSB and XY phase because an impractically large bond dimension is needed to accurately extract the simultaneous $\chi, |i - j| \to \infty$ limit of $\langle S_i^+ S_j^-\rangle$. The white line denoting the boundary of the AFM phase is from Fig. 3(a). (b) Spin-wave excitation density $\langle a_i^\dagger a_i\rangle$ calculated using Eq. (13) for $N = 1001$ spins. For $J_z > \zeta(\alpha)/\eta(\alpha)$ imaginary frequencies appear in the Bogoliubov spectrum, indicating a classical instability toward the AFM phase. We set $\langle a_i^\dagger a_i\rangle = 1$ in this region, as well as in regions where $\langle a_i^\dagger a_i\rangle > 1$. For $\alpha > 3$, $\langle a_i^\dagger a_i\rangle \to \infty$ as $N \to \infty$, thus no CSB phase is expected (boundary shown by the white dashed line).

the long-range ferromagnetic order along the x direction is destroyed by quantum fluctuations in the thermodynamic limit; we expect that $\lim_{|i-j|\to\infty} \langle S_i^+ S_j^-\rangle = 0$, and the system will be disordered (either Haldane or XY). For $\alpha < 3$, we find that $[1 - \mu^2(q)/\omega^2(q)]^{-1/2} \propto |q|^{-(\alpha-1)/2}$ to leading order in q, and the integral is infrared convergent. The excitation density $\langle a_i^\dagger a_i\rangle$ converges to a finite constant, so we expect a CSB phase with $\lim_{|i-j|\to\infty} \langle S_i^+ S_j^-\rangle \neq 0$. However, when $\langle a_i^\dagger a_i\rangle$ converges to a constant on the order of 1, the spin-wave approximation is not expected to be accurate, and it is possible

that the actual ground state of H remains disordered for α slightly less than 3.

For $J_{xy} = 1$, classically the spins prefer to anti-align in the $x - y$ plane. Expanding around this classical state with the same spin-wave approximation, both $\mu(q)$ and $\omega(q)$ become fully analytic due to an additional alternating sign $(-1)^r$ in Eqs. (11) and (12). As a result, $[1 - \mu^2(q)/\omega^2(q)]^{-1/2}$ always exhibits a $|q|^{-1}$ divergence at small q, and continuous symmetry breaking is forbidden for all $\alpha > 0$.

From our infinite-size DMRG calculations, we see that $\langle S_i^+ S_j^- \rangle \sim 1/|i-j|^\eta$ decays with a rather slow power law in the XY phase (e.g. $\eta = 0.25$ at $J_z = 0$ and $\alpha = \infty$; η is non-universal and depends on J_z and α). At the maximum separation that we can calculate accurately, $\langle S_i^+ S_j^- \rangle$ only shows a crossover from the XY phase to the CSB phase [Fig. 4(a)]. This crossover can in fact be qualitatively reproduced using the above spin-wave theory by calculating the spin-wave excitation density $\langle a_i^\dagger a_i \rangle$ for a finite system size [Fig. 4(b)].

Further numerical evidence of the CSB phase is obtained by calculating the effective central charge c_{eff} as a function of α and J_z, which can be obtained by calculating the half-chain entanglement entropy S for two chains with different total lengths N_1 and N_2 using a finite-size DMRG algorithm. Explicitly, for large N_1 and N_2, we have

$$c_{\text{eff}} \approx 6 \frac{S(N_1) - S(N_2)}{\ln(N_1) - \ln(N_2)}. \tag{14}$$

In the XY phase (including its boundaries) and at the boundary between the Haldane and AFM phases, we expect 1+1D conformal symmetry in the underlying field theory model [56, 58], with c_{eff} being the actual central charge representing the conformal anomaly [78]. In the Haldane, FM, and AFM phases, no 1+1D conformal symmetry exists due to the presence of a gap. Although the CSB phase is gapless, we expect a breakdown of 1+1D conformal symmetry due to the $1/r^\alpha$ long-range interactions that become relevant in the RG sense for $\alpha \lesssim 3$ [32, 34, 69]. We emphasize that in phases with no conformal symmetry, c_{eff} does not have the meaning of the central charge and is used only as a diagnostic here to numerically find phase boundaries.

We identify the XY-to-CSB phase boundary in Fig. 5 as the place where c_{eff} starts to become appreciably (5-10%) larger than 1. Due to finite-size effects, c_{eff} changes continuously for continuous phase transitions, and we are not able to obtain the precise location of the XY-to-CSB phase boundary. Nevertheless, we find good agreement with the XY-to-CSB phase boundary predicted by spin-wave theory, especially near $J_z = -1$, where spin-wave theory should be almost exact. Together with perturbative field theory calculations presented in Ref. [69], we expect the phase boundary in Fig. 5 to be accurate within a few percent. A CSB-XY-Haldane tricritical point is found at $\alpha \approx 2.75$ and $J_z \approx 1.35$.

From Ref. [69], it follows that the XY-to-CSB transition is a BKT-like transition that belongs to a universality class different from the XY-to-Haldane BKT transition. The Haldane-to-CSB transition is somewhat exotic, because the Haldane phase maps to a high-temperature disordered phase in a 2D classical model [82], and *in the absence of long-range interactions*, the CSB phase exists in 2D only at zero temperature [2] and is unlikely to undergo a phase transition directly to a high-temperature disordered phase. We also argue that the CSB-to-Haldane transition is not described by a 1+1D CFT, as supported by our numerical calculations shown in Fig. 5(b), where c_{eff} changes smoothly (at least for finite chains) from a value larger than 1 to 0 during the CSB-to-Haldane transition.

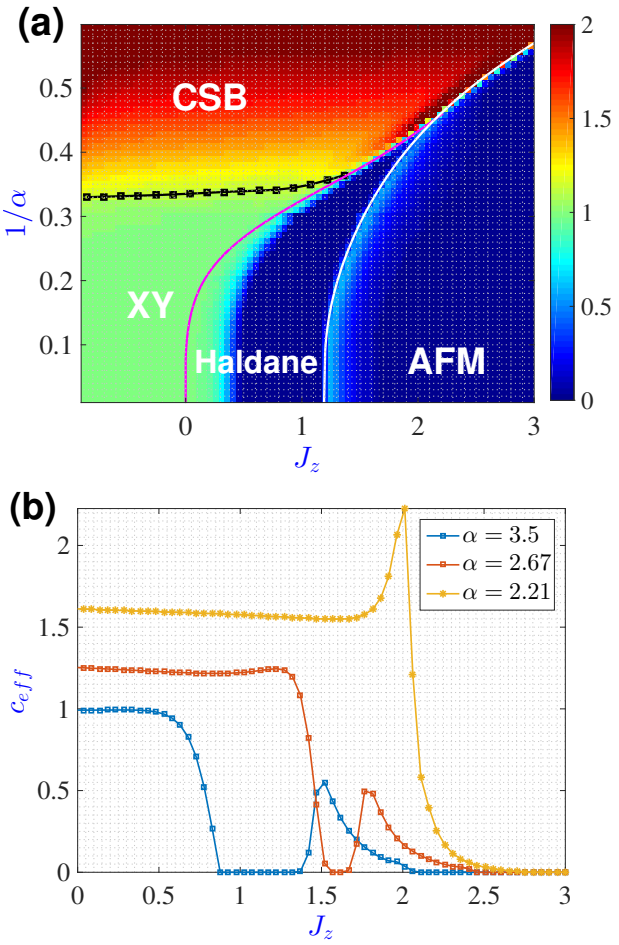

Figure 5: Calculation of the effective central charge c_{eff} as a function of J_z and α for $J_{xy} = -1$, extracted from finite-size DMRG calculations with $N_1 = 100$, $N_2 = 110$, and a maximum bond dimension of 500. (a) The black squares (fitted by the black line) show where c_{eff} starts to deviate from 1 when going from the XY to the CSB phase. The purple line and white line are from Fig. 3, and show the boundaries of the Haldane phase. (The calculation of c_{eff} is inaccurate in predicting the location of the XY-to-Haldane transition due to strong finite-size effects [50, 75–77].) For better contrast, locations with $c > 2$ are shown with the color corresponding to $c = 2$. (b) For our finite-size chains, the XY-to-Haldane BKT phase transition is signaled by a continuous drop of c_{eff} from 1 to 0 ($\alpha = 3.5$). The Haldane-to-AFM phase transition is identified by a peak with value around 0.5 in c_{eff} ($\alpha = 3.5$ and $\alpha = 2.67$). The CSB-to-Haldane transition is expected to be continuous and not associated with a central charge ($\alpha = 2.67$). The CSB-to-AFM transition has a sharp peak in c_{eff} ($\alpha = 2.21$), an indication of a first-order transition [56].

The CSB-to-AFM phase transition is very likely to be first-order, similar to the transition between the large-D and AFM phases studied in Refs. [55, 64], despite the existence of quantum fluctuations in both phases. As shown in Fig. 5, we observe a sharp peak in c_{eff} at small αs when J_z is varied, indicating a first order transition [56], with further evidence that includes jumps in sub-lattice magnetization and spin-spin correlation across the CSB-to-AFM transition (not shown).

V. EXPERIMENTAL DETECTION

It was theoretically proposed in Refs. [43, 44] that the Hamiltonian we consider can be simulated (for widely tunable J_z and $0 < \alpha < 3$) by using microwave field gradients or optical dipole forces to induce spin-spin interactions in a chain of trapped ions. The simulation of Eq. (1) with $J_{xy} = 1$ and $J_z = 0$ was experimentally demonstrated for a few ions with α tuned around 1 [45], where the ground state was adiabatically prepared by slowly ramping down an extra single-ion anisotropy term $D(t)\sum_i (S_i^z)^2$, with $D(t) > 0$. As the system size increases, the energy gap separating the ground state from the rest of the spectrum will become progressively smaller near the point where a phase transition between the "large-D" phase and the XY/Haldane/FM/AFM phase occurs in the thermodynamic limit [64]. To avoid a slow ground state preparation process, we can adiabatically ramp down a staggered magnetic field in the z direction, $h(t)\sum_{i=1}^{N}(-1)^i S_i^z$, with $h(t) > 0$ [43, 44]. By preparing an initial state that is the highest excited state of the staggered field Hamiltonian, the same adiabatically ramping process will lead us to the ground state of the Hamiltonian Eq. (1) with the opposite sign of both J_{xy} and J_z. As discussed in Ref. [44], the spin correlation functions $\langle S_i^z S_j^z\rangle$ and the string-order correlation $\mathcal{S}_{ij}^z \equiv \langle S_i^z S_j^z \prod_{i<k<j}(-1)^{S_k^z}\rangle$ can be measured in trapped-ion experiments for any two ions i and j. Together with arbitrary single-spin rotations performed with microwave or optical Raman transitions, we can measure these correlations along any direction. Near-future experiments will most likely be limited to a few tens of spins. Although this limitation makes it difficult to probe continuous phase transitions, one can nevertheless observe important signatures of all five phases discussed in the manuscript by tuning J_z/J_{xy} and α deep into each phase. These signatures are summarized below and shown in Fig. 6.

FM phase [Fig. 6(a)]: Within the FM phase, $\langle S_i^z S_j^z\rangle = 1$ and $\langle S_i^x S_j^x\rangle = 0$ for any i and j, thus confirming perfect alignment of spins along the z direction.

AFM phase [Fig. 6(b)]: For sufficiently large $J_z > 0$, we have $\langle S_i^z S_j^z\rangle \approx (-1)^{i-j}$, showing a near perfect anti-alignment of spins along the z direction. In contrast, $\langle S_i^x S_j^x\rangle$ vanishes over a separation of just a few sites.

Haldane phase [Fig. 6(c)]: $\mathcal{S}_{ij}^z$ converges quickly to a nonzero constant as $|i-j|$ increases. In contrast, $\langle S_i^z S_j^z\rangle$ and $\langle S_i^x S_j^x\rangle$ vanishe over a separation of just a few sites.

XY phase [Fig. 6(d)]: We consider the XY phase for $J_{xy} = 1$ since the XY phase hardly exist for $\alpha < 3$ and $J_{xy} = -1$. $\mathcal{S}_{ij}^z$ and $\langle S_i^z S_j^z\rangle$ both decay quickly to zero as $|i-j|$ increases. $\langle S_i^x S_j^x\rangle$ oscillates and its amplitude decays very slowly (the slow decay reflects a relatively small value of the critical exponent associated with the correlation function decay).

CSB phase [Fig. 6(f)]: As in the XY phase, both $\mathcal{S}_{ij}^z$ and $\langle S_i^z S_j^z\rangle$ decay quickly to zero. However, $\langle S_i^x S_j^x\rangle$ converges quickly to approximately 0.5 at large $|i-j|$, showing a near perfect ordering of spins in the $x-y$ plane. Note that we are not explicitly breaking $U(1)$ symmetry here, so $\langle S_i^x S_j^x\rangle = \langle S_i^y S_j^y\rangle = \frac{1}{2}\langle S_i^+ S_j^-\rangle$. This is done because it is desirable for the experiment to operate within the $\sum_{i=1}^{N} S_i^z = 0$ subspace, where magnetic field noise and unwanted phonon couplings are suppressed [44, 45].

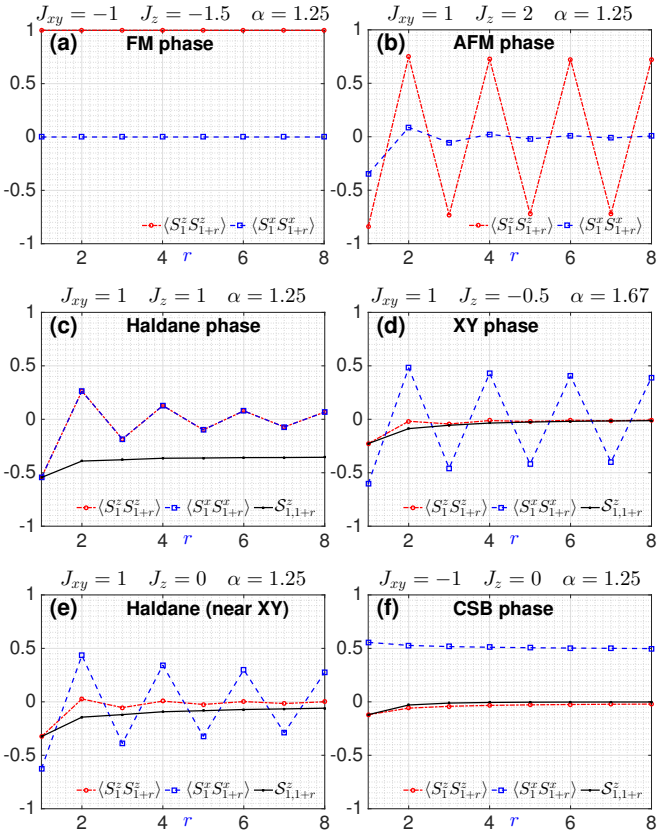

Figure 6: Signatures of all five phases for a $N = 16$ spin chain. Except for (e), we tune J_{xy}, J_z and α to set the ground state deep into each phase. Each phase is distinguished from the other phases by different behaviors in various spin-spin correlation functions.

Finally, we point out that, even in the experimental setup already demonstrated in Ref. [45], for which $J_z = 0$, one can still explore the two most interesting phases studied in this manuscript: the Haldane phase and the CSB phase. Note that, for $J_{xy} = 1$, $J_z = 0$ lies close to the Haldane-to-XY phase boundary, and thus one observes signatures of both phases, as in Fig. 6(e).

VI. CONCLUSION AND OUTLOOK

By tuning the anisotropy $J_z/|J_{xy}|$ and the power-law exponent α, we have explored a rich variety of quantum phases—and the transitions between them—in a long-range interacting spin-1 XXZ chain. For $J_{xy} = -1$, long-range interactions give rise to a rather unusual phase diagram due to the emergence of a continuous symmetry breaking phase in one spatial dimension. Because the CSB phase cannot happen in short-range interacting 1D spin-system, the nature of the phase transitions into and out of it is rather interesting; an in-depth study of the universality class of the CSB-to-XY transition was carried out in a separate work [69], where a similar transition in the long-range interacting spin-1/2 XXZ chain is analyzed. On the other hand, the CSB-to-Haldane transition, absent in spin-1/2 chains, requires further study to be understood thoroughly. The CSB-Haldane-AFM tricritical point is reminiscent of the tricritical point at the intersection of the large-D, Haldane and AFM phases, which has been related to the integrable Takhtajan-Babujian model described by an $SU(2)_2$ Wess-Zumino-Witten (WZW) model with central charge $c = 3/2$ [56, 89–92]. Additional numerical calculations are needed to accurately determine the central charge at the CSB-Haldane-AFM tricritical point. Generalizations of our model to include single-ion anisotropy and a magnetic field are readily achievable in current trapped-ion experiments [44, 45]. Understanding these exotic quantum phase transitions—induced by long-range interactions that are highly tunable in current experiments—requires the confrontation of numerous theoretical and numerical challenges, and motivates experimental quantum simulation of the model using AMO systems.

Acknowledgements

We thank G. Pupillo, D. Vodola, L. Lepori, A. Turner, J. Pixley, M. Wall, P. Hess, A. Lee, J. Smith, A. Retzker and I. Cohen for helpful discussions. This work was supported by the ARO, the AFOSR, NSF PIF, NSF PFC at the JQI, and the ARL. M. F.-F. thanks the NRC for support.

* Electronic address: gzx@umd.edu

[1] S. Sachdev, *Quantum phase transitions*, 2nd ed. (Cambridge University Press, 2011).
[2] N. D. Mermin and H. Wagner, Phys. Rev. Lett. **17**, 1133 (1966).
[3] F. D. M. Haldane, Phys. Lett. A **93**, 464 (1983).
[4] F. D. M. Haldane, Phys. Rev. Lett. **50**, 1153 (1983).
[5] F. Pollmann, E. Berg, A. M. Turner, and M. Oshikawa, Phys. Rev. B **85**, 075125 (2012).
[6] X. Chen, Z.-C. Gu, Z.-X. Liu, and X.-G. Wen, Phys. Rev. B **87**, 155114 (2013).
[7] P. Di Francesco, P. Mathieu, and D. Sénéchal, *Conformal field theory*, Graduate texts in contemporary physics (Springer, New York, 1997).
[8] I. Bloch, J. Dalibard, and W. Zwerger, Rev. Mod. Phys. **80**, 885 (2008).
[9] K. Kim, M.-S. Chang, S. Korenblit, R. Islam, E. E. Edwards, J. K. Freericks, G.-D. Lin, L.-M. Duan, and C. Monroe, Nature **465**, 590 (2010).
[10] I. Bloch, J. Dalibard, and S. Nascimbène, Nat. Phys. **8**, 267 (2012).
[11] J. W. Britton, B. C. Sawyer, A. C. Keith, C.-C. J. Wang, J. K. Freericks, H. Uys, M. J. Biercuk, and J. J. Bollinger, Nature **484**, 489 (2012).
[12] B. Yan, S. A. Moses, B. Gadway, J. P. Covey, K. R. A. Hazzard, A. M. Rey, D. S. Jin, and J. Ye, Nature **501**, 521 (2013).
[13] D. Peter, S. Müller, S. Wessel, and H. P. Büchler, Phys. Rev. Lett. **109** (2012).
[14] J. S. Douglas, H. Habibian, C.-L. Hung, A. V. Gorshkov, H. J. Kimble, and D. E. Chang, Nature Photon. **9**, 326 (2015).
[15] P. Jurcevic, B. P. Lanyon, P. Hauke, C. Hempel, P. Zoller, R. Blatt, and C. F. Roos, Nature **511**, 202 (2014).
[16] K. R. Hazzard, B. Gadway, M. Foss-Feig, B. Yan, S. A. Moses, J. P. Covey, N. Y. Yao, M. D. Lukin, J. Ye, D. S. Jin, and A. M. Rey, Phys. Rev. Lett. **113**, 195302 (2014).
[17] A. de Paz, A. Sharma, A. Chotia, E. Maréchal, J. H. Huckans, P. Pedri, L. Santos, O. Gorceix, L. Vernac, and B. Laburthe-Tolra, Phys. Rev. Lett. **111**, 185305 (2013).
[18] P. Richerme, Z.-X. Gong, A. Lee, C. Senko, J. Smith, M. Foss-Feig, S. Michalakis, A. V. Gorshkov, and C. Monroe, Nature **511**, 198 (2014).
[19] P. Schauß, M. Cheneau, M. Endres, T. Fukuhara, S. Hild, A. Omran, T. Pohl, C. Gross, S. Kuhr, and I. Bloch, Nature **491**, 87 (2012).
[20] S. R. Manmana, E. M. Stoudenmire, K. R. A. Hazzard, A. M. Rey, and A. V. Gorshkov, Phys. Rev. B **87**, 081106 (2013).
[21] N. Y. Yao, C. R. Laumann, A. V. Gorshkov, S. D. Bennett, E. Demler, P. Zoller, and M. D. Lukin, Phys. Rev. Lett. **109**, 266804 (2012).
[22] N. Y. Yao, A. V. Gorshkov, C. R. Laumann, A. M. Läuchli, J. Ye, and M. D. Lukin, Phys. Rev. Lett. **110**, 185302 (2013).
[23] M. E. Fisher, S.-k. Ma, and B. G. Nickel, Phys. Rev. Lett. **29**, 917 (1972).
[24] S. A. Cannas and F. A. Tamarit, Phys. Rev. B **54**, R12661 (1996).
[25] E. Luijten and H. W. J. Blöte, Phys. Rev. B **56**, 8945 (1997).
[26] H. G. Katzgraber and A. P. Young, Phys. Rev. B **72**, 184416 (2005).
[27] A. Campa, T. Dauxois, and S. Ruffo, Phys. Rep. **480**, 57 (2009).
[28] T. Koffel, M. Lewenstein, and L. Tagliacozzo, Phys. Rev. Lett. **109**, 267203 (2012).
[29] R. Bachelard and M. Kastner, Phys. Rev. Lett. **110**, 170603 (2013).
[30] J. Eisert, M. van den Worm, S. R. Manmana, and M. Kastner, Phys. Rev. Lett. **111**, 260401 (2013).
[31] Z.-X. Gong, M. Foss-Feig, S. Michalakis, and A. V. Gorshkov, Phys. Rev. Lett. **113**, 030602 (2014).
[32] D. Vodola, L. Lepori, E. Ercolessi, A. V. Gorshkov, and G. Pupillo, Phys. Rev. Lett. **113**, 156402 (2014).
[33] M. Foss-Feig, Z.-X. Gong, C. W. Clark, and A. V. Gorshkov, Phys. Rev. Lett. **114**, 157201 (2015).
[34] D. Vodola, L. Lepori, E. Ercolessi, and G. Pupillo, arXiv:1508.00820 (2015).
[35] M. F. Maghrebi, Z.-X. Gong, M. Foss-Feig, and A. V. Gorshkov, arXiv:1508.00906 (2015).
[36] M. A. Rajabpour and S. Sotiriadis, Phys. Rev. B **91**, 045131

(2015).
[37] M. B. Hastings and T. Koma, Commun. Math. Phys. **265**, 781 (2006).
[38] M. G. Nezhadhaghighi and M. A. Rajabpour, Phys. Rev. B **88**, 045426 (2013).
[39] M. G. Nezhadhaghighi and M. A. Rajabpour, EPL **100**, 60011 (2012).
[40] N. Laflorencie, I. Affleck, and M. Berciu, J. Stat. Phys. **2005**, P12001 (2005).
[41] A. W. Sandvik, Phys. Rev. Lett. **104** (2010).
[42] T. Blanchard, M. Picco, and M. A. Rajabpour, EPL **101**, 56003 (2013).
[43] I. Cohen and A. Retzker, Phys. Rev. Lett. **112**, 040503 (2014).
[44] I. Cohen, P. Richerme, Z.-X. Gong, C. Monroe, and A. Retzker, Phys. Rev. A **92**, 012334 (2015).
[45] C. Senko, P. Richerme, J. Smith, A. Lee, I. Cohen, A. Retzker, and C. Monroe, Phys. Rev. X **5**, 021026 (2015).
[46] Z.-X. Gong, M. F. Maghrebi, A. Hu, M. L. Wall, M. Foss-Feig, and A. V. Gorshkov, arXiv:1505.03146 (2015).
[47] M. Kac, G. E. Uhlenbeck, and P. C. Hemmer, J. Math. Phys. **4**, 216 (1963).
[48] For an infinite system, the energy renormalization may change the system from gapped to gapless.
[49] T. Kennedy and H. Tasaki, Comm. Math. Phys. **147**, 431 (1992).
[50] A. Kitazawa, K. Nomura, and K. Okamoto, Phys. Rev. Lett. **76**, 4038 (1996).
[51] M. Tsukano and K. Nomura, Phys. Rev. B **57**, R8087 (1998).
[52] K. Nomura, Phys. Rev. B **40**, 9142 (1989).
[53] T. Sakai and M. Takahashi, J. Phys. Soc. Jpn. **59**, 2688 (1990).
[54] Y. H. Su, S. Young Cho, B. Li, H.-L. Wang, and H.-Q. Zhou, J. Phys. Soc. Jpn. **81**, 074003 (2012).
[55] G.-H. Liu, W. Li, W.-L. You, G. Su, and G.-S. Tian, Physica B **443**, 63 (2014).
[56] S. Ejima and H. Fehske, Phys. Rev. B **91** (2015).
[57] H. J. Schulz, Phys. Rev. B **34**, 6372 (1986).
[58] F. C. Alcaraz and A. Moreo, Phys. Rev. B **46**, 2896 (1992).
[59] K. Nomura, J. Phys. A **28**, 5451 (1995).
[60] K. Nomura and A. Kitazawa, J. Phys. A **31**, 7341 (1998).
[61] A. Kitazawa, K. Hijii, and K. Nomura, J. Phys. A: Math. Gen. **36**, L351 (2003).
[62] R. Botet and R. Jullien, Phys. Rev. B **27**, 613 (1983).
[63] H. Ueda, H. Nakano, and K. Kusakabe, Phys. Rev. B **78**, 224402 (2008).
[64] W. Chen, K. Hida, and B. C. Sanctuary, Phys. Rev. B **67**, 104401 (2003).
[65] K. Nomura and K. Okamoto, J. Phys. Soc. Jpn. **62**, 1123 (1993).
[66] P. Bruno, Phys. Rev. Lett. **87**, 137203 (2001).
[67] A. M. Lobos, M. Tezuka, and A. M. García-García, Phys. Rev. B **88**, 134506 (2013).
[68] M. Tezuka, A. M. García-García, and M. A. Cazalilla, Phys. Rev. A **90**, 053618 (2014).
[69] M. F. Maghrebi, Z.-X. Gong, and A. V. Gorshkov, arXiv:1510.01325 (2015).
[70] U. Schollwöck, Ann. Phys. **326**, 96 (2011).
[71] G. M. Crosswhite, A. C. Doherty, and G. Vidal, Phys. Rev. B **78**, 035116 (2008).
[72] M. L. Wall and L. D. Carr, New J. Phys. **14**, 125015 (2012).
[73] Our MPS code is largely based on the open source MPS project at http://sourceforge.net/projects/openmps/. The $1/r^\alpha$ interaction is represented as a matrix product operator by fitting the power law to a sum of exponentials [71].
[74] I. P. McCulloch, arXiv:0804.2509 (2008).
[75] A. L. Malvezzi and F. C. Alcaraz, J. Phys. Soc. Jpn. **64**, 4485 (1995).
[76] R. R. P. Singh and M. P. Gelfand, Phys. Rev. Lett. **61**, 2133 (1988).
[77] F. C. Alcaraz and Y. Hatsugai, Phys. Rev. B **46**, 13914 (1992).
[78] P. Calabrese and J. Cardy, J. Stat. Mech. **2004**, P06002 (2004).
[79] I. Affleck, Phys. Rev. Lett. **54**, 966 (1985).
[80] Here the expression are for non-integer α. For integer α, the expressions are slightly different but cause no important changes to the discussion below.
[81] E. S. Sorensen and I. Affleck, Phys. Rev. B **49**, 13235 (1994).
[82] E. Fradkin, *Field theories of condensed matter physics*, 2nd ed. (Cambridge University Press, 2013).
[83] E. Brézin and J. Zinn-Justin, eds., *Fields, strings and critical phenomena: Les Houches, session XLIX, 1988* (North-Holland, 1990).
[84] S. R. White, Phys. Rev. Lett. **69**, 2863 (1992).
[85] S. R. White and D. A. Huse, Phys. Rev. B **48**, 3844 (1993).
[86] T. Murashima, K. Hijii, K. Nomura, and T. Tonegawa, J. Phys. Soc. Jpn. **74**, 1544 (2005).
[87] Note that gapped phases with sufficiently long-ranged interactions can violate entanglement area law [28, 32, 34], but this has not been observed in our model.
[88] A. Auerbach, *Interacting electrons and quantum magnetism*, Graduate texts in contemporary physics (Springer-Verlag, New York, 1994).
[89] A. M. Tsvelik, Phys. Rev. B **42**, 10499 (1990).
[90] A. Kitazawa and K. Nomura, Phys. Rev. B **59**, 11358 (1999).
[91] C. Degli Esposti Boschi, E. Ercolessi, F. Ortolani, and M. Roncaglia, EPJ B **35**, 465 (2003).
[92] J. H. Pixley, A. Shashi, and A. H. Nevidomskyy, Phys. Rev. B **90**, 214426 (2014).